Arabian Journal of Chemistry (2022) **15**, 103604

King Saud University

Arabian Journal of Chemistry

www.ksu.edu.sa
www.sciencedirect.com

ORIGINAL ARTICLE

Preparation of photoluminescent nanocomposite ink toward dual-mode secure anti-counterfeiting stamps

Khlood Abou-Melha

Chemistry Department, Faculty of Science, King Khalid University, Abha, Saudi Arabia

Received 19 October 2021; accepted 2 December 2021
Available online 8 December 2021

KEYWORDS

Lanthanide-doped aluminate;
Dual-mode;
Photochromism;
Fluorescence;
Security encoding

Abstract Fluorescent photochromism has been applied as an attractive approach for the production of effective authentication substrates to show dual-mode secure encoding. In the current study, novel photochromic and fluorescent nanocomposite ink was developed to introduce a stamped film with strong dual-mode emission for anti-counterfeiting purposes. Inorganic/organic nanocomposite ink was developed from lanthanide-doped aluminate (LDA) dispersed in poly(acrylic acid)-based binder. To produce a transparent film, LDA must be dispersed well in the poly(acrylic acid)-based ink solution. The fluorescent and photochromic nanocomposite ink was stamped effectively onto cellulose documents followed with thermal fixation. Homogeneous fluorescent and photochromic layer was stamped onto paper surface providing a transparent look with the ability to switch to green beneath ultraviolet as illustrated by CIE Lab. The stamped documents were studied by photoluminescence spectra to show an absorption peak at 364 nm, and fluorescence band at 438 nm. The induced security encoding was transparent beneath visible light turning into visible greenish-yellow beneath ultraviolet light indicating a bathochromic shift. LDA was synthesized in the nanoparticle form and characterized by transmission electron microscopy (TEM), X-ray diffraction (XRD) and energy-dispersive X-ray spectroscopy (EDS). The morphological properties of the stamped documents were examined by infrared spectroscopy (FTIR), scan electron microscope (SEM), EDS, and X-ray fluorescence (XRF). The stamped paper sheets displayed an efficiently reversible photochromism without fatigue under visible and ultraviolet lights. The rheologies of the prepared photoluminescent nanocomposite inks as well as the mechanical performance of the stamped sheets were investigated.

1. Introduction

Counterfeiting of currency, foodstuff, and branded commodities has been a universal crisis, causing massive economy and security implications for governments, consumers and industrial sectors (Abdollahi et al., 2020; Abdollahi and Dashti, 2021; Muthamma et al., 2021; Abdollahi et al., 2020). The size of the underground economy reached billions of dollars due to

E-mail address: dr.khlood@hotmail.com
Peer review under responsibility of King Saud University.

Production and hosting by Elsevier

https://doi.org/10.1016/j.arabjc.2021.103604
1878-5352

counterfeiting. The vital need for the development of a new generation of high-tech anti-counterfeiting systems has recently induced extensive research on advanced anti-counterfeiting materials. The optical property has been reported as an ideal security element in the anti-counterfeiting systems due to their ability of being easy-to-authenticate and hard-to-copy (Azimi et al., 2021; Kumar et al., 2017; Singh et al., 2017; Wu et al., 2021; Sheng et al., 2014). The optically active anticounterfeiting materials, like Plasmonic nanomaterials and quantum dots have been efficiently developed. Those materials usually exhibit small and uniform particle size as well as high fluorescence efficiency, proposing great potential in the anti-counterfeiting applications (Skwierczyńska et al., 2020). However, the anti-counterfeiting optical information in those materials depends mostly on highly short fluorescence emission leading to serious background emission interferences from the printing media, such as banknotes. Thus, the development of efficient materials with long-persistent fluorescence (i.e. phosphorescence) is quite significant for the preparation of advanced anti-counterfeiting commodities without background fluorescence interference (Monica et al., 2021). The improvement of security authentication has been recently highly significant challenge for a variety of documents, like certificates, passports, banknotes and identification cards. Hence, numerous traditional authentication techniques were explored like digital, ink and paper methods. The recent authentication models included quick responding codes, radio frequency ID cards and holographic labeling (Muthamma et al., 2020; Yu et al., 2021). Nonetheless, these authentication models are complicated and costly. Thus, a wide range of photo-responsive materials, such as upconversion nanoparticles, supramolecular scaffolds and polymer dots, have been developed to provide anticounterfeiting inks for printing secure patterns (Abdollahi et al., 2020). These photochromic materials were printed as solvent and aqueous formulae onto cellulosic substrates. Photochromism is a light-driven reversible phenomenon between two forms of different colors because those two forms have different absorbance and/or emission spectra (Li et al., 2019). Photochromism has been an interesting technology for a variety of of smart commodities, such as smart packaging, smart displays, optical data storage, memories, sensors, camouflage for military applications, sunglasses and ophthalmic lenses. Anticounterfeiting polymer inks were widely studied owing to their high durable and stable optical properties. Most of anticounterfeiting polymer inks use polymer nanoparticles able to show excellent optical characteristics owing to their large surface area and low light reflection (Wei et al., 2020; Yu et al., 2021). Plugging the printer nozzles due to agglomeration of those polymer nanoparticles has been a critical confrontation. Therefore, the development of luminescent nanoparticles dispersed in a polymer matrix can be described as an alternative technology toward improved authentication patterns (Ren et al., 2019).

Organic photochromic dyes, primarily spirooxazine-based colorants, have been used to create photochromic materials. Photochromic organic dyes usually suffer a number of drawbacks, such as molecular degradation, low dye uptake, poor dye diffusion into the fibrous matrix, increasing the matrix hardness, poor photostability and high cost compared to inorganic pigments (Yuan et al., 2019). Microencapsulation methods have been used to solve some of these drawbacks by turning dyes into pigments. This approach improves the stability of photochromic compounds, but it also adds roughness and stiffness to the treated material. The steric hindrance caused by molecular switching activity usually results in total inhibition of photochromis limiting the use of photochromic organic dyes (Li et al., 2017; Al-Qahtani et al., 2021). With an extended exposure to light, organic dyes lose their photochromic and luminous visual properties indicating poor durability. Photochromic inorganic dyes, on the other hand, are very stable and inexpensive. Because of their tiny molecular structure, the inorganic dyes have a fast rate of dye diffusion. Due to the fact that the emission property relies on an electron excitation and relaxation process, they do not suffer steric hindrance effects making them very photostable and highly durable providing smooth and flexible photochromic surfaces with high emission quantum yield (Al-Qahtani et al., 2021; Khattab et al., 2021; Al-Qahtani et al., 2021). Photoluminescent inorganic nanomaterials with long-persistent phosphorescence have been interesting research due to their significant uses in many fields, like biological imaging, sensors and light-emitting diodes. Nowadays, the most common lanthanide-doped photoluminescent nanomaterials are inorganic phosphors, such as $CaAl_2O_4$: Eu^{2+}, Nd^{3+} and $SrAl_2O_4$: Eu^{2+}, Dy^{3+} (Ashwini et al., 2021). Lanthanide-doped aluminates (LDAs) have been particularly significant luminescent pigments that have been widely employed in the preparation of various photochromic materials, like chemosensors. This could be ascribed to their quick response, high reversibility, photo-switchable emission and photostability (Baatout et al., 2019). LDAs have showed an emissive colorimetric switch under visible/UV irradiation. The utilization of LDAs for anti-counterfeiting purposes has been a growing field owing to their photostability, durability and luminous efficiency. Many lanthanide-doped phosphorescent pigments of various colors have been developed, such as $CaAl_2O_4$: Eu^{2+},Nd^{3+} for preliminary blue emission, $SrAl_2O_4$:Eu^{2+}, Dy^{3+} for preliminary greenish emission, and CaS: Eu^{2+},Tm^{3+},Ce^{3+} for preliminary red emission (Hu et al., 2018; Abdelhameed et al., 2021; Zhang et al., 2020). However, LDAs have been distinctive materials as a result of their unique features, such as photostability, non-toxicity, non-radioactivity, high brightness, recyclability and thermal stability. Thus, the preparation of UV-induced photochromic and fluorescent LDA-containing nanocomposite inks is a smart strategy toward the preparation of cheap anti-counterfeiting materials with high durability (Ma et al., 2019). Those features open new horizons to develop authenticated merchandise of high efficiency and stability. Nonetheless, the particulate mold technique of photoluminescent substances is a typical method as it limits their applications. Therefore, the nano-sized particles of photoluminescent substances have been integrated into various inorganic/organic materials to defeat the weak mechanical performance of the developed LDA-immobilized films (Calderón-Olvera et al., 2018). Poly(acrylic acid) (PAA) is a colorless and hygroscopic homopolymer derived from free radical polymerization of acrylic acid. PAA has been used in a diversity of products like superabsorbent, cosmetics, floor cleaner, disposable diapers, detergent and dispersing agent. The neutralized PAA organo-

gels have been appropriate biocompatible matrices for pharmaceutical purposes, such as skin care products. Thus, PAA could be employed as a proper supporting substrate for the development of nanocomposite inks immobilized with LDA nanoparticles (Melo et al., 2018; Aminyan and Bazgir, 2019). Khattab et al. reported recently various studies on the preparation of photochromic textile fibers immobilized with LDA (Khattab, 2020).

Herein, we have successfully prepared a series of color tunable and photostable nanocomposite inks from different concentrations of LDA nano-scale particles dispersed in a medium of polyacrylic acid to function as an authentication stamp for a variety of products, such as documents, certificates, passports, banknotes and identification cards. The prepared fluorescent and photochromic dual-mode nanocomposite inks demonstrated different optical properties relying on the applied ratio of LDA nanoparticles. The stamped film demonstrated transparent appearance beneath visible light and long-lived photoluminescent green color beneath ultraviolet supply. Therefore, the stamped paper is protected from scratching and erasing, and replacement with other counterfeiting composites. The dual-mode fluorescent photochromism based authentication composite ink was developed by admixing poly(acrylic acid) as crosslinkable binder matrix with LDA nanoparticles as the photochromic agent. The thermofixation process was applied to crosslink the poly(acrylic acid) binding agent to generate thin film on the document surface with the LDA nanoparticles entrapped within this film. The morphologies and chemical structures of LDA particles were evaluated by TEM and EDXA, respectively. On the other hand, the morphologies, elemental contents and optical activity were explored by different analytical techniques, including SEM, EDXA, photoluminescence spectra and CIE Lab studies. The rheologies of prepared nanocomposite ink and mechanical performance of the stamped papers were also explored. The stamped films demonstrated ultraviolet-induced dual-mode photochromic and fluorescent phenomenon, which has been suitable technology to offer anti-counterfeiting security patterns with green-yellow shade beneath UV source without trace underneath visible light. The present approach can be described as an efficient technique to produce many authentication commodities with strong optical dual-mode photo-responsiveness toward a better marketplace to avoid counterfeit and poor commodities that have been a threat to society.

2. Experimental details

2.1. Chemicals and materials

The synthesis of LDA ($SrAl_2O_4$: Eu^{2+}, Dy^{3+}) was carried out using previous procedure (high temperature solid state method) (Abumelha, 2021) starting from Sr(II) carbonate (Aldrich), Al(III) oxide (Merck), boric acid (Merck), Dy(III) oxide (Sigma-Aldrich), and Eu(III) oxide (Merck). Poly(acrylic acid) binder additive was obtained from Dystar, Egypt. An off-white Wahttman paper sheets (Sigma-Aldrich) were applied as documents for the stamping process of patterns. Wahttman paper exhibiting a pore size of 11 μm was employed.

2.2. Methods and apparatus

Photoluminescence spectra of the stamped samples were studied with JASCO FP6500 (Japan) coupled to phosphorescence accessories to study decaying time. Decaying was investigated by irradiation for 15 min by an ultraviolet supply which was blocked-up using a blockade to allow collecting the results. An external ultraviolet source (6 Watt) was employed as an external illumination supply at 365 nm. JEOL 1230 TEM (Japan) was employed to inspect the morphology of LDA particles using a dispersion of LDA in acetone previously homogenized (35 kHz) for 15 min. XRD diagram of LDA was inspected on Bruker Advance D-8 (Germany) utilizing copper (Kα) radiation (1.5406 Å). Infrared spectral curves were reported using Nexus 670 (Nicolet, United States). Both morphologies and elemental contents of LDA as well as the authentication films stamped onto paper surface was studied on SEM Quanta FEG250 (Czech Republic) connected to TEAM-EDXA mapping. The chemical contents of the authentication films stamped onto sheet surface were also evaluated by advanced sequential AXIOS XRF. The rheological performance of the nanocomposite ink was evaluated by DVIII Brookfield Rheometer to determine viscosity upon changing shear rate. The mechanical properties of the stamped paper sheets at different concentrations of LDA nanoparticles were studied on Zwick-Universal (load cell of 100 N). Triple Roll Mill ES80 was applied to crush LDA microparticles into nano-scale particles (16–26 nm).

2.3. Synthesis of LDA nano-scale particles

The synthesis of LDA ($SrAl_2O_4$: Eu^{2+}, Dy^{3+}) was performed using the high temperature solid state method (Abumelha, 2021). A dispersion of Eu(III) oxide (0.02 mol), Sr(II) carbonate (1 mol), Dy(III) oxide (0.03 mol), aluminium oxide (2 mol), and boric acid (0.2 mol) in ethanol homogenized (35 kHz) over 30 min, exposed to heat at 90 °C for 22 hrs, and grinding over 2 hrs. In a reduction carbon atmosphere, the generated adduct was sintered at ~ 1300 °C over ~ 2.5 hrs, subjected to milling and sieving to provide microparticles of LDA (13–34 μm). LDA nanoparticles were developed using the top-down technique (Garrigue et al., 2004) by charging 10 g of LDA powder into a vial of ball mill (20 cm) attached to an oscillating disc. SiC ball mill (0.1 cm) was subjected to persistent collisions with both vibrating disc and vial containing LDA powder for 24 hrs to afford LDA nanoparticles.

2.4. Preparation and application of inks

An admixture of diammonium phosphate (1 % w-w) as a dispersing agent, NH_4OH (1 % w-w) to adjust pH of solution, and poly(acrylic acid) as a binding material (15 % w-w) was dissolved in distilled water (83%). The solution was exposed to mechanical stirring over 30 min to allow a homogeneous dispersion. Several solutions were then developed from the above prepared solution by dispersing different quantities of LDA nanoparticles, including zero, 0.05, 0.10, 0.25, 0.50, 0.75, 1.00, 1.25 and 1.50 % w-w. The admixtures were subjected to continuous stirring for 30 min, and then exposed to ultrasonic (25 kHz) over 60 min to achieve uniform dispersion. The nanocomposite inks showed an off-white viscous milky

fluid. The nanocomposite inks were directly stamped onto paper sheets using a wooden stamp. The stamped sheets were air-dried for 5 min, and then subjected to thermal fixation at 145 °C over 3 min. The developed stamped sheets were abbreviated by symbols from Stamp-0 to Stamp-8, respectively.

2.5. Reversibility and durability

The stamped sheet was exposed to ultraviolet light source (365 nm; 5 min) at 5 cm above the sheet. The sheet was then inserted into a dark wood box for 15 min to recover its origin state. The above procedure was performed a number of cycles, and the luminescence spectra were recorded for every cycle.

2.6. Colorimetric studies

To investigate transparency and colorimetric switching, both K/S and CIE Lab of the stamped films were evaluated before and after exposure to ultraviolet light using UltraScanPro (Hunter Lab, USA). The optical transmittance of the stamped films was examined by ultraviolet–visible HITACHI U-3010. Photographic images of the stamped paper sheet were obtained by Canon A710IS.

3. Results and discussion

3.1. Preparation of photochromic stamp

LDA was prepared according to previous literature approach (Abumelha, 2021). The generated LDA powder demonstrated a micro-scale size (13–34 μm); thus, the top-down approach was utilized to give the desired LDA nano-scale particles (Garrigue et al., 2004). LDA was studied by TEM and selected area electron diffraction to signify diameters of 16–26 nm as illustrated in Fig. 1. Different quantities of LDA nanoparticles were then admixed with separate solutions of low molecular weight poly(acrylic acid) dispersed in distilled water to give viscous mixtures. Poly (acrylic acid) was employed as a binding agent. Diammonium phosphate acted as a dispersing agent, whereas ammonium hydroxide was added to adjust pH of solution. The mixtures were subjected to continuous mechanical stirring and strong homogenization to warranty a consistent dispersion. The developed nanocomposite inks exhibited an off-white milky solution. The nanocomposite inks were applied directly onto the cellulosic sheet by a wooden stamp, and then subjected to thermofixation at 145 °C.

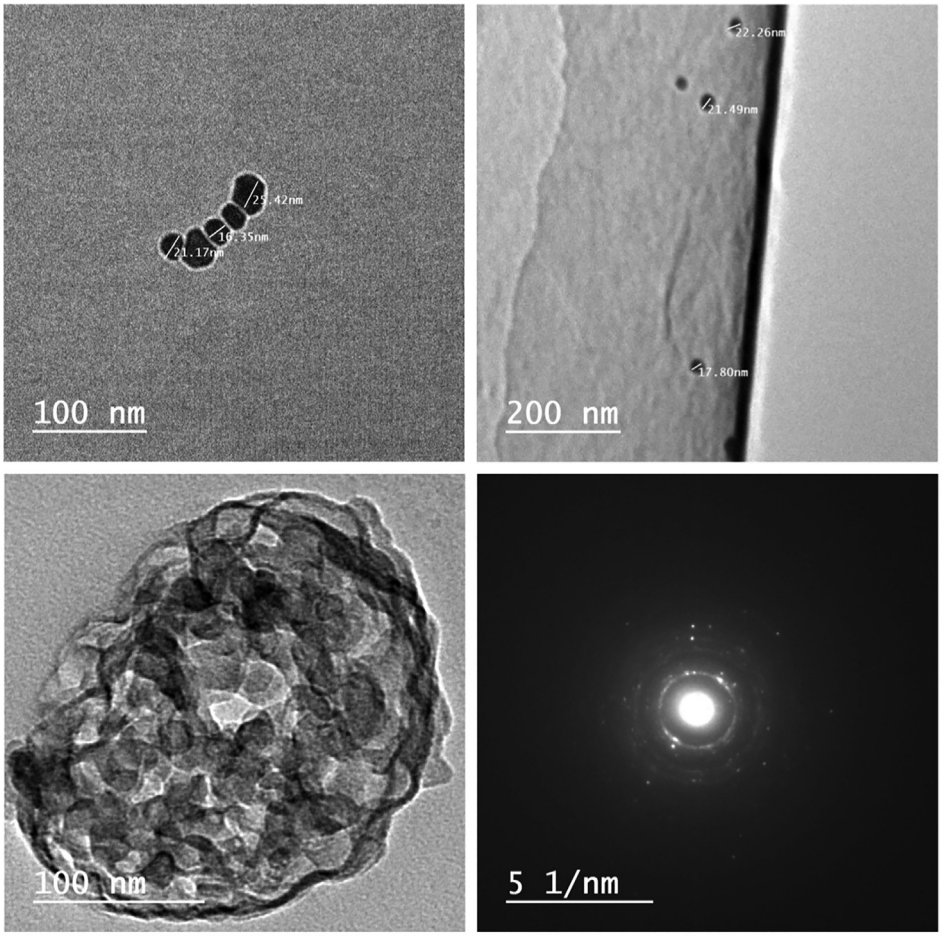

Fig. 1 TEM graphs of LDA nanoparticles.

The chemical composition of LDA was proved by EDX and elemental mapping to indicate high purity as shown in Fig. 2**a-b**. XRD diagram of LDA nanoparticles **(**Fig. 2**c)** demonstrated pure LDA signals matching with the monoclinic $SrAl_2O_4$ (JCPDS card number. 74/0794) to designate low temperature monoclinic phase of LDA nano-sized particles (Khattab et al., 2021). No other crystalline phases were detected that both Eu^{2+} and Dy^{3+} are completely embedded in the crystal lattice of $SrAl_2O_4$ (Khattab et al., 2021; Devi et al., 2020). This also verified that the low lanthanides ratios had no effect on the $SrAl_2O_4$ phase composition.

3.2. Morphologies of stamped sheets

Smart products are known as materials with the ability to switch their properties, such as color, responding to an external stimulus, such as light. Photochromic composites have been reported as intelligent materials with the ability to change their colors in response to light. Photochromic-based authentication of documents has attracted much interest due to its promising applications, such as passports, national identification cards and banknotes. The utilization of nano-scale phosphor particles results in an enhanced homogeneous dispersal of LDA particles within poly(acrylic acid) film bulk stamped onto paper sheet (Atta, 2021). Fig. 3 and Table 1 demonstrate the morphologies and elemental compositions of the stamped photochromic film onto paper sheets. SEM images showed an efficient deposition of LDA nanoparticles onto paper surface. The stamped samples displayed no main differences with increasing LDA ratio. However, the amount of LDA particles between fibers of paper morphological structure was found to increase with increasing LDA in ink formulations. SEM proved an efficient homogeneous dispersal of LDA onto paper surface, which could be ascribed to the coordination binding of aluminium as an elemental component of LDA with the hydroxyl oxygen electrons lone pairs of electrons of cellulosic structure. LDA nanoparticles were approximately between 16 and 26 nm, which resulted in a homogeneous dispersion in the ink composite; and consequently a homogeneous distribution onto paper surface. The ammonium hydroxide aqueous solution provides an alkaline environment to cellulose to facilitate the dissociation of the hydroxyl substituents to generate a negatively charged cellulose surface. Therefore, the positively charged pigment can be easily attracted by the negatively charged paper surface. In comparison to blank sheet, no physical changes were detected on the stamped paper. Additionally, both EDX and elements maps proved a consistent distribution of LDA within PAA layer stamped onto paper sheet (Table 1). Both carbon and oxygen demonstrated major contents because they are major constituents in paper sheets as well as PAA. On

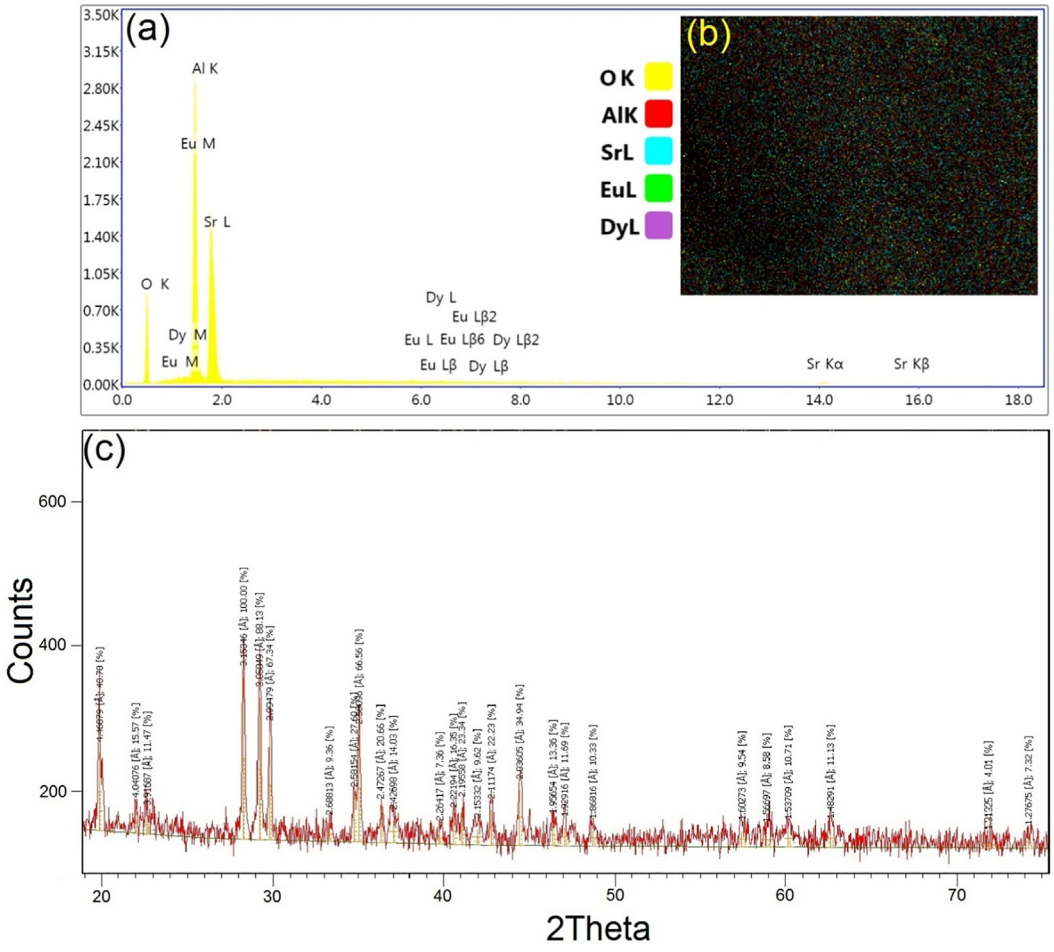

Fig. 2 EDX diagram (a), elements mapping (b), and XRD pattern (c) of LDA nanoparticles.

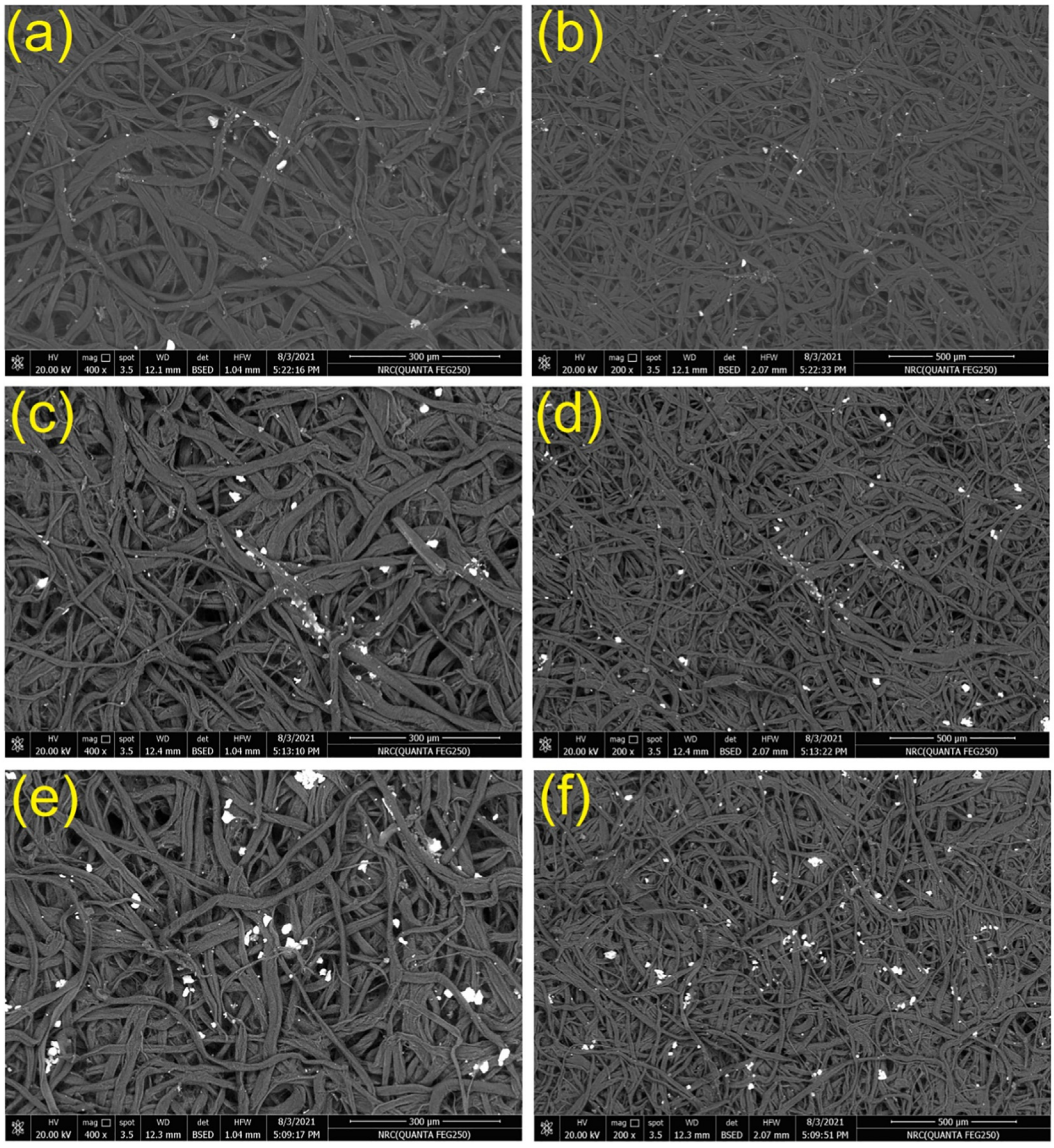

Fig. 3 SEM graphs of Stamp-1 (a), Stamp-5 (b) and Stamp-8 (c); the density of LDA nanoparticles on the paper sheet surface increases with increasing the ratio of LDA nanoparticles in the ink formula.

the other hand, Al, Sr, Dy and Eu displayed the minor contents of the stamped layer.

The elemental contents and distribution were evaluated by EDX at three different areas on the surfaces of both unstamped and stamped paper sheets (Table 1). EDX proved the elemental contents of paper sheets indicating that carbon and oxygen are the major contents, whereas aluminum, strontium, europium and dysprosium are the minor contents of the stamped documents. The elemental ratios at the three scanned areas were approximately identical to verify even spreading of LDA on the stamped sheet surface. XRF was also employed to find out the elemental ratios of the stamped sheet as indicated in Table 2. EDX is an appropriate analytical approach to identify the chemical compositions with extremely low errors. On the other side, XRF provides an elemental identification approach as low as 10 mg/kg (Carmona et al., 2010). Thus, XRF offers an incomplete detection of elements. XRF of the

Table 1 Elemental compositions of stamped documents inspected by EDX at three different areas (a_1, a_2 and a_3) on the paper surafce.

Sheet		C	O	Al	Sr	Eu	Dy
Stamp-0		51.15	48.85	0	0	0	0
Stamp-1	a_1	51.12	47.46	0.77	0.44	0.13	0.08
	a_2	51.43	47.11	0.83	0.37	0.16	0.10
	a_3	51.37	47.18	0.70	0.53	0.15	0.07
Stamp-5	a_1	50.24	47.54	1.03	0.62	0.35	0.22
	a_2	50.33	47.40	1.11	0.58	0.39	0.19
	a_3	50.29	47.46	1.02	0.75	0.32	0.16
Stamp-8	a_1	49.05	47.80	1.45	0.95	0.44	0.31
	a_2	49.30	47.54	1.57	0.86	0.48	0.25
	a_3	49.28	47.57	1.43	1.02	0.46	0.24

Table 2 Chemical composition of stamped documents as reported by XRF.

Analyte	Oxide	Elemental ratio			
		Stamp-1	Stamp-4	Stamp-6	Stamp-8
Ca	CaO	8.12	7.82	6.93	5.93
Al	Al_2O_3	39.25	40.86	43.56	45.69
Sr	SrO	17.63	18.71	21.40	22.81
Mg	MgO SiO_2	7.56	6.97	5.65	4.94
Si	Cl	9.19	8.87	7.58	6.95
Cl	Na_2O	6.43	5.94	4.75	4.37
Na	K_2O	6.48	5.99	5.88	5.46
K		5.34	4.84	4.25	3.85

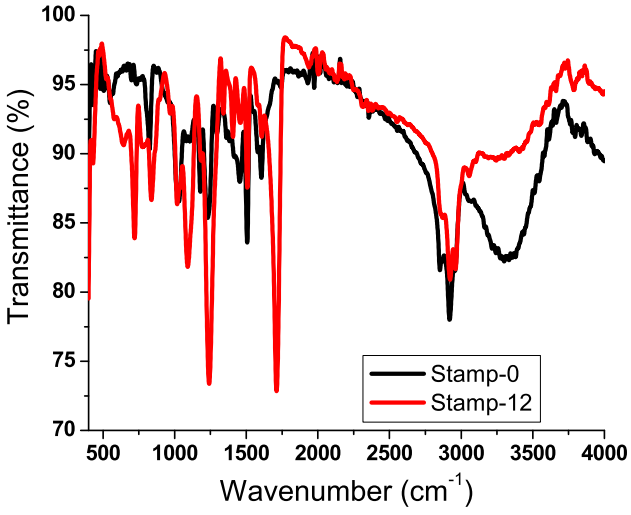

Fig. 4 Infrared spectra of stamped paper sheets.

stamped sheets detected the existence of Sr and Al; however, the very low ratios of Dy and Eu were not detected. The chemical content of the stamped paper sheets tested by EDX and XRF were in agreement with the percents used in the preparation of LDA and luminescent sheets. The mapping micrographs proved both chemical compositions of the stamped sheets and the uniform distribution of LDA onto the luminescent stamped sheets.

Infrared analysis has been one of the most spectroscopic techniques used to study the functional groups on an organic material. Herein, infrared analysis was employed to examine the binding mechanism of the luminescent composite ink onto the paper sheet as illustrated in Fig. 4. Cellulose is a natural biopolymer bearing hydroxyl groups proved by the band detected at 3328 cm^{-1}. The aliphatic substituents were proved by the band at 2922 cm^{-1}. After the thermal fixation of LDA-integrated into poly(acrylic acid) layer deposited onto the paper surface, a strong binding occurs between the hydroxyl groups on cellulose and the carboxylic groups on PAA binder. An absorbance band was monitored at 1723 cm^{-1} for carbonyl ester of PAA (Hill et al., 2019). The hydroxyl intensity monitored at 3309 was found to decrease after stamping owing to formation of ester bonding among the carboxyl substituents on PAA and the hydroxyl groups on cellulose. The aliphatic stretch intensity monitored at 2922 cm^{-1} was monitored to decrease with increasing LDA. Likewise, the aliphatic bending band reported at 1245 cm^{-1} also decreased with increasing the ratio of LDA (Khattab et al., 2019). Additional bands were observed at 431, 644 and 714 cm^{-1} due to the lattice vibrating bonds of SrO, OAlO and AlO (Hameed et al., 2021), respectively.

3.3. Photochromism studies

Facile technology was developed for the production of smart authentication stamp with the capability to change color beneath ultraviolet rays. Photo-responsive nanocomposite ink was synthesized using lanthanide-doped aluminate nanoparticles, poly(acrylic acid) binder, diammonium phosphate and ammonium hydroxide. LDA functioned as filler within the poly(acrylic acid) binding agent which functioned as a trapping bulk which crosslinked on the paper surface by thermal fixation. The stamped paper sheets displayed reversible luminescence. However, the stamped sheets with LDA content higher than 0.75% showed slower reversibility (i.e. phosphorescence) compared to the stamped sheets with LDA content lower than 0.75% (i.e. fluorescence). Thus, the stamped sheets with LDA content higher than 0.75% exhibit long-lived phosphorescence. All stamped sheets exhibited the same emission at 438 nm, which is extremely less than that of LDA powder (519 nm) (Al-Qahtani et al., 2021). Stamp-0 demonstrated an off-white shade acting as an efficient background improving the naked-eye recognition of the photochromic effect (Fig. 5). Testing of the stamped sheets demonstrated an off-white shade similar to Stamp-0 beneath daylight and greenish-yellow beneath UV supply, which can be identified as a dual-mode secure fluorescent photochromism.

The strength of the LDA emission intensity has been previously reported as a concentration-dependent phenomenon (Khattab et al., 2021). This was proved with the increased excitation energy with increasing LDA ratio (Fig. 6**a**). All stamped

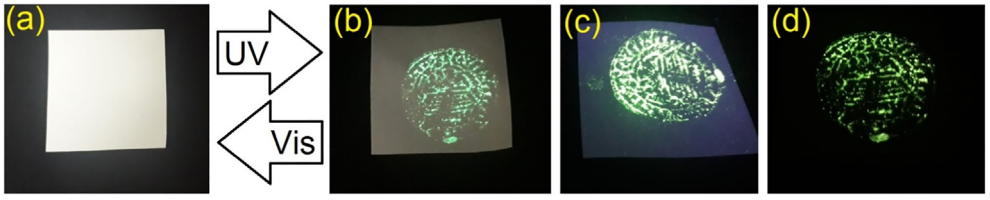

Fig. 5 Photochromism of Stamp-5 displaying colorimetric exchange from off-white beneath daylight (a) to weak green color beneath ultraviolet supply (b; 254 nm), strong green color beneath ultraviolet supply (c; 365 nm), and greenish-yellow for a few seconds in a dark wooden box (d).

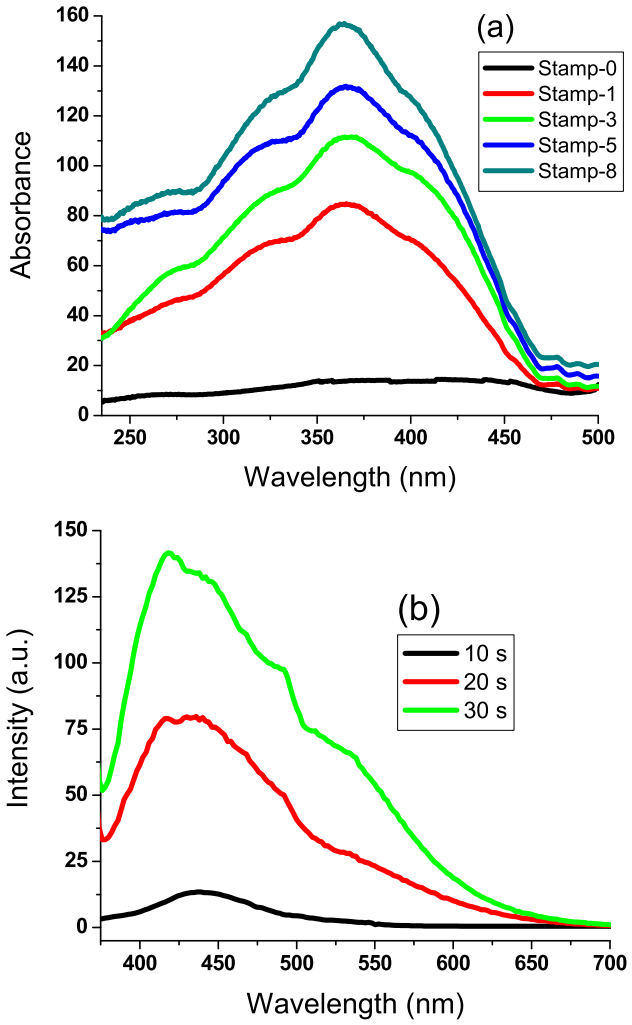

Fig. 6 Excitation spectra of some selected stamped sheets with different rations of LDA (a); and emission curves of Stamp-5 versus the irradiation time from 10 to 30 s (b).

sheets exhibited an instant and reversible photochromism beneath ultraviolet supply. However, the stamped sheets with low LDA content equal to or less than 0.75% developed a quick reversibility indicating fluorescence emission. The sheets with LDA ratio higher than 0.75% developed long-lived phosphorescence owing to their slow reversibility. Therefore, Stamp-5 displayed the strongest fluorescent photochromism in comparison to samples with low LDA content which displayed weak greenish-yellow emission.

Thus, according to the photochromic results, Stamp-5 represents the best fitting (optimized) composite ink. The emission spectra were studied against the irradiation time. As illustrated in Fig. 6**b**, strong absorbance band was observed in the ultraviolet range at 364 nm due to Eu^{2+}. The emission peak was detected at 438 nm due Eu^{2+} proving a total exchange of Eu^{3+} to Eu^{2+} (Khattab et al., 2020). Therefore, the emission spectra are assigned to $4f^{6}5D^{1} \leftrightarrow 4f^{7}$ transition of Eu^{2+} proving that the light absorbed by Dy^{3+} was transfered to Eu^{2+} (Abumelha, 2021). The key purpose of Dy^{3+} is to promote the formation of traps to release the stored light under darkness leading to relaxation of Eu^{2+} to the ground state (Abdelhameed et al., 2021). The gradual increase of the irradiation time results in gradual increase of the emission intensity at 438 nm associated with a band shift to 418 nm. The excitation intensity was also monitored to increase with increasing the ratio of LDA to indicate a greener color. Similarly, the emission intensity increased with increasing the irradiation time to indicate a greener color. Decay time profile displayed a nonlinear relation against time demonstrating initially quick decay followed by slower decaying as illustrated in Fig. 7.

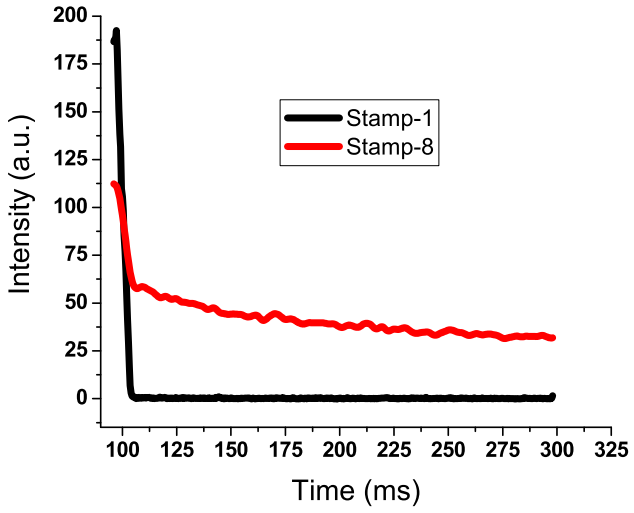

Fig. 7 Decay time profiles of stamped sheets; Stamp-1 and Stamp-8.

The resistance to fatigue and photostability of the stamped paper sheet (Stamp-5) were assessed by running a repetitive process of irradiation with ultraviolet supply and then exposure to darkness for several cycles as illustrated in Fig. 8. Stamp-5 was exposed to UV to show a greenish color, and after that exposed to darkness to regain back its native off-white color. The fluorescence intensities were recorded for each round to prove approximately the same magnitude verifying high photostability and resistance to fatigue.

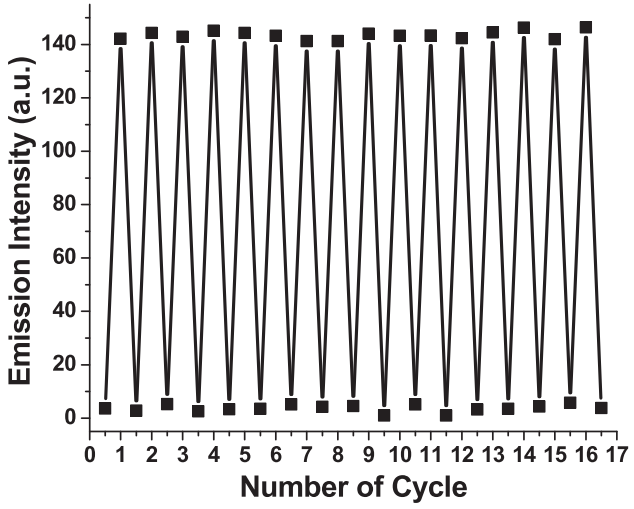

Fig. 8 Emission intensity of Stamp-5 at 418 nm (irradiation time 30 s).

Table 3 Colorimetric screening of blank and stamped sheets at different conents of LDA beneath ultraviolet (UV) and daylight (DL).

Sheet	*K*/*S*		a*		b*		L*	
	DL	UV	DL	UV	DL	UV	DL	UV
Stamp-0	1.18	1.26	0.04	0.09	1.37	1.48	93.07	93.18
Stamp-1	1.32	1.93	−1.67	−7.21	1.71	4.65	92.60	89.23
Stamp-2	1.46	2.06	−1.56	−7.89	1.82	4.43	92.41	86.78
Stamp-3	1.59	2.74	−1.52	−8.43	2.05	6.53	92.25	84.65
Stamp-4	1.72	3.42	−1.48	−10.00	2.36	8.31	91.77	83.34
Stamp-5	1.89	3.80	−1.36	−11.40	2.48	9.55	91.28	81.06
Stamp-6	2.07	4.05	−1.31	−13.68	2.57	10.58	90.43	79.68
Stamp-7	2.20	4.57	−1.27	−14.30	2.62	10.66	89.65	77.84
Stamp-8	2.38	4.91	−1.15	−16.58	2.79	11.73	89.14	74.89

3.4. Colorimetric results

Colorimetric properties were studied to evaluate photochromism of the stamped paper sheets. The color switch under visible and ultraviolet lights was studied by CIE Lab parameters as displayed in Table 3. Both blank and stamped sheets possessed the same off-white color to prove the deposition of a transparent photochromic film onto the paper surface. Both blank and stamped sheets demonstrated no significant changes in CIE Lab and *K*/*S* with increasing LDA to verify transparency of the photochromic film deposited onto the stamped sheets. This can be ascribed to the extremely low quantities of LDA immobilized into the stamped film. Slight changes were observed in *K*/*S* beneath UV light in comparison to daylight vision. Nonetheless, L* decreased upon exposure to ultraviolet light to indicate a chromogenic exchange from off-white to greenish-yellow. The low -a* and low + b* increased beneath ultraviolet rays. The increased -a* signifies a colorimetric switch to green. The increased + b* signifies a colorimetric switching to yellow. Therefore, the stamped sheets instantaneously switched their colors from off-white to greenish-yellow beneath ultraviolet supply. Additionally, the stamped sheets showed higher a* in comparison to b*. This can be ascribed to the high contribution arising from the greenish hue in comparison to the contribution of yellowish hue. L* decreased, whereas *K*/*S*, a* and b* increased under ultraviolet light with raising LDA to denote increasing the ratio of the green color.

3.5. Mechanical and rheological properties

The rheological properties of the nanocomposite ink (Stamp-5) were investigated as shown in Fig. 9. The composite ink was not highly thick because its flowing plot was found to best fitting Newton's law. The viscosity was monitored to decrease rapidly and linearly with increasing the shear rate. The viscosity decreased quickly to reach equilibrium at low and high shear rates.

Compared to Stamp-0, tensile and Young's modulus of Stamp-1 decreased close to strain percent because Young's modulus relies on strain/tensile. PAA binding agent as a main constituent of composite ink stamped on paper sheet demonstrated adhesion and elasticity on the stamped sheet to prove an enhanced strain percent. Fig. 10 demonstrates the mechanical properties of stamped sheets at various ratios of LDA. Young's modulus and Tensile increased upon elevating LDA ratio from Stamp-0 to Stamp-6, and then continue nearly with the same value with raising LDA ratio from Stamp-6 to Stamp-8. This could be attributed to the increased spaces between fibers owing to coagulating LDA particles. However, negligible variations were observed in strain percent at break with increasing LDA ratio due to the interfacial cross-linking among the positively charged LDA and negative charges of cellulose surface. The negative charges on cellulose were formed via deprotonation of the hydroxyl group upon curing with NH_4OH. Thus, the inclusion of LDA improved the crosslinking process between fibers (Abdelhameed et al., 2021).

4. Conclusion

Novel dual-mode fluorescent and photochromic nanocomposite ink was stamped onto cellulose sheet was developed to demonstrate a chromogenic switch from off-white beneath sunlight to green-yellow beneath UV supply. Lanthanide-doped aluminate phosphor nanoparticles were established to be a practical material to assemble nanocomposite ink for dual-mode secure anticounterfeiting stamp. The present strategy can be used to produce facile and cheap authentication stamp with high durability, photostability and good mechani-

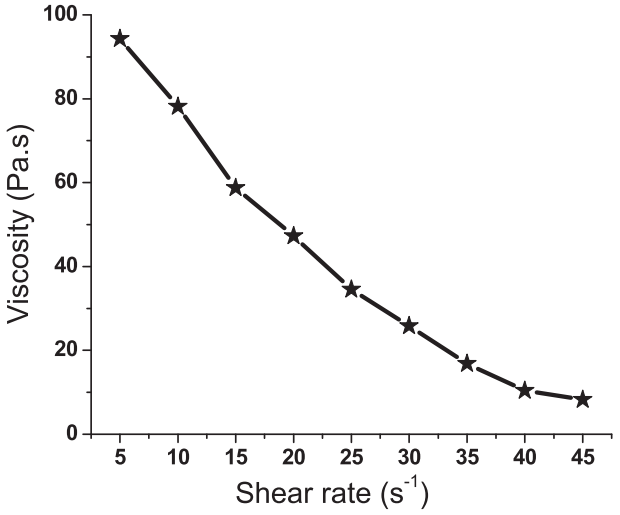

Fig. 9 Viscosity of composite ink against shear rates.

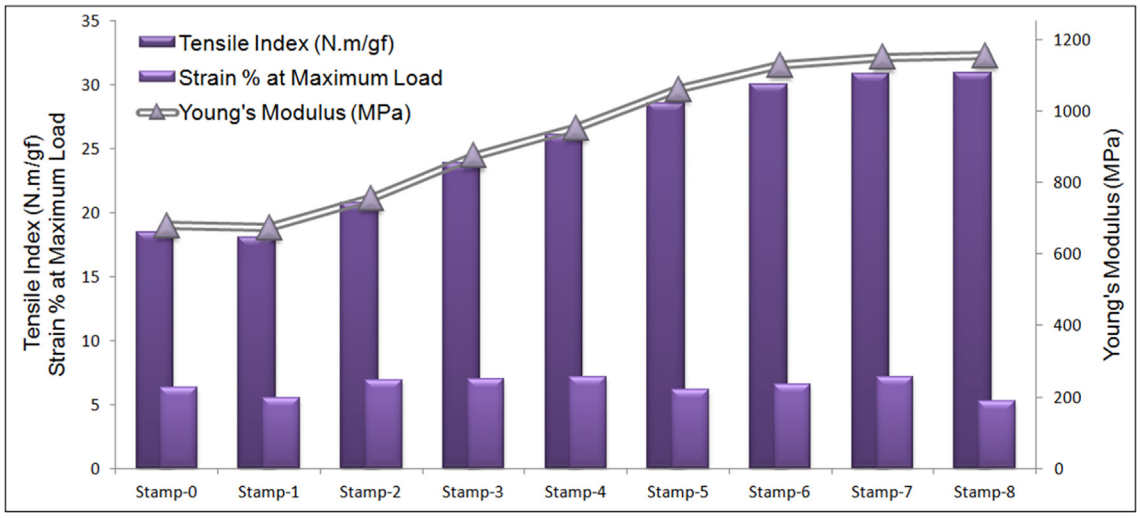

Fig. 10 Effects of LDA content on mechanical activity of stamped sheets.

cal properties. The nanocomposite ink was developed by mixing the lanthanide-doped aluminate phosphor with a poly (acrylic acid) binder to fasten the phosphor particles onto the sheet surface. The best fluorescent photochromism was assigned to the stamped sheet with LDA ratio of 0.75%, which demonstrated the highest green fluorescence. The stamped sheets showed absorbance at 364 nm and fluorescence wavelength at 438 nm. Transparency of stamped layer was accomplished by allowing homogeneous distribution of the pigment nano-scale particles within the bulk of the binding agent. The morphology of pigment was verified by EDX, XRD and TEM to display a particle size of 16–26 nm. The stamped paper sheets were studied by SEM, EDX, XRF, IR, luminescence spectra and CIE Lab parameters. Under visible daylight, the composite films exhibited a transparent appearance on the off-white documents. Those composite films developed a dual-mode fluorescent photochromism by changing color to greenish-yellow beneath ultraviolet light. In this context, the current anti-counterfeiting transparent composite film can be easily applied onto a diversity of commercial commodities, such as banknotes and brand protection.

Declaration of Competing Interest

The authors declare that they have no known competing financial interests or personal relationships that could have appeared to influence the work reported in this paper.

References

Abdollahi, A., Herizchi, A., Roghani-Mamaqani, H., Alidaei-Sharif, H., 2020. Interaction of photoswitchable nanoparticles with cellulosic materials for anticounterfeiting and authentication security documents. Carbohydrate polymers 230, 115603.

Abdollahi, A., Dashti, A., 2021. Photoluminescent Nanoinks with Multilevel Security for Quick Authentication of Encoded Optical Tags by Sunlight: Effective Physicochemical Parameters on Responsivity, Printability, and Brightness. ACS Applied Materials & Interfaces 13 (37), 44878–44892.

Muthamma, K., Sunil, D., Shetty, P., Kulkarni, S.D., Anand, P.J., Kekuda, D., 2021. Eco-friendly flexographic ink from fluorene-based Schiff base pigment for anti-counterfeiting and printed electronics applications. Progress in Organic Coatings 161, 106463.

Abdollahi, A., Roghani-Mamaqani, H., Salami-Kalajahi, M., Razavi, B., 2020. Encryption and authentication of security patterns by ecofriendly multi-color photoluminescent inks containing oxazolidine-functionalized nanoparticles. Journal of Colloid and Interface Science 580, 192–210.

Azimi, R., Abdollahi, A., Roghani-Mamaqani, H., Salami-Kalajahi, M., 2021. Dual Mode Security Anticounterfeiting and Encoding by Electrospinning of Highly Photoluminescent Spiropyran Nanofibers. Journal of Materials Chemistry C 9, 9571–9583.

Kumar, P., Nagpal, K., Gupta, B.K., 2017. Unclonable security codes designed from multicolor luminescent lanthanide-doped Y2O3 nanorods for anticounterfeiting. ACS applied materials & interfaces 9 (16), 14301–14308.

Singh, Varun Kumar, Ramesh Kumar Chitumalla, Sai Kishore Ravi, Yaoxin Zhang, Yongjie Xi, Vijayvenkataramana Sanjairaj, Chun Zhang, Joonkyung Jang, and Swee Ching Tan. "Inkjet-printable hydrochromic paper for encrypting information and anticounterfeiting." *ACS applied materials & interfaces* 9, no. 38 (2017): 33071-33079.

Wu, Y., Zhao, X., Zhang, Z., Xiang, J., Suo, H., Guo, C., 2021. Dual-mode dichromatic SrBi4Ti4O15: Er3 + emitting phosphor for anticounterfeiting application. Ceramics International 47 (11), 15067–15072.

Sheng, Lan, Minjie Li, Shaoyin Zhu, Hao Li, Guan Xi, Yong-Gang Li, Yi Wang et al. "Hydrochromic molecular switches for water-jet rewritable paper." *Nature communications* 5, no. 1 (2014): 1-8.

Skwierczyńska, M., Woźny, P., Runowski, M., Perzanowski, M., Kulpiński, P., Lis, S., 2020. Bifunctional magnetic-upconverting luminescent cellulose fibers for anticounterfeiting purposes. Journal of Alloys and Compounds 829, 154456.

Monica, J.H., Ratna, J.S., Dave, P.Y., 2021. Anticounterfeiting Technology–A Luminescent Path: Short Review. Journal of Advanced Chemical Sciences, 706–710.

Muthamma, K., Sunil, D., Shetty, P., 2020. "Luminophoric organic molecules for anticounterfeit printing ink applications: an up-to-date review." *Materials Today*. Chemistry 18, 100361.

Yu, X., Zhang, H., Jihong, Y.u., 2021. Luminescence anti-counterfeiting: From elementary to advanced. Aggregate 2 (1), 20–34.

Abdollahi, A., Roghani-Mamaqani, H., Razavi, B., Salami-Kalajahi, M., 2020. Photoluminescent and chromic nanomaterials for anticounterfeiting technologies: recent advances and future challenges. ACS nano 14 (11), 14417–14492.

Li, Z., Wang, G., Ye, Y., Li, B., Li, H., Chen, B., 2019. Loading photochromic molecules into a luminescent metal–organic framework for information anticounterfeiting. Angewandte Chemie 131 (50), 18193–18199.

Wei, T., Jia, B., Shen, L., Zhao, C., Liwei, W.u., Zhang, B., Tao, X., Shengcheng, W.u., Liang, Y., 2020. Reversible upconversion modulation in new photochromic SrBi2Nb2O9 based ceramics for optical storage and anti-counterfeiting applications. Journal of the European Ceramic Society 40 (12), 4153–4163.

Yu, C.-M., Wang, P.-H., Liu, Q., Cai, L.-Z., Guo, G.-C., 2021. Modulating Fading Time of Photochromic Compounds by Molecular Design for Erasable Inkless Printing and Anti-counterfeiting. Crystal Growth & Design 21 (2), 1323–1328.

Ren, Y., Yang, Z., Li, M., Ruan, J., Zhao, J., Qiu, J., Song, Z., Zhou, D., 2019. Reversible upconversion luminescence modification based on photochromism in BaMgSiO4: Yb3+, Tb3+ ceramics for anti-counterfeiting applications. Advanced Optical Materials 7 (15), 1900213.

Yuan, J., Yuan, Y., Tian, X., Wang, H., Liu, Y., Feng, R., 2019. Photoswitchable boronic acid derived salicylidenehydrazone enabled by photochromic spirooxazine and fulgide moieties: multiple responses of optical absorption, fluorescence emission, and quadratic nonlinear optics. The Journal of Physical Chemistry C 123 (49), 29838–29855.

Li, X., Li, C., Wang, S., Dong, H., Ma, X., Cao, D., 2017. Synthesis and properties of photochromic spirooxazine with aggregation-induced emission fluorophores polymeric nanoparticles. Dyes and Pigments 142, 481–490.

Al-Qahtani, S.D., Binyaseen, A.M., Aljuhani, E., Aljohani, M., Alzahrani, H.K., Shah, R., El-Metwaly, N.M., 2021. Production of smart nanocomposite for glass coating toward photochromic and long-persistent photoluminescent smart windows. Ceramics International 48 (1), 903–912.

Khattab, T.A., El-Naggar, M.E., Abdelrahman, M.S., Aldalbahi, A., Hatshan, M.R., 2021. Facile development of photochromic cellulose acetate transparent nanocomposite film immobilized with lanthanide-doped pigment: ultraviolet blocking, superhydrophobic, and antimicrobial activity. Luminescence 36 (2), 543–555.

Al-Qahtani, S., Aljuhani, E., Felaly, R., Alkhamis, K., Alkabli, J., Munshi, A., El-Metwaly, N., 2021. Development of Photoluminescent Translucent Wood toward Photochromic Smart Window Applications. Industrial & Engineering Chemistry Research 60 (23), 8340–8350.

Ashwini, K.R., Premkumar, H.B., Daruka Prasad, B., Darshan, G.P., Nagabhushana, H., Sharma, S.C., Prashantha, S.C., 2021. Green emitting SrAl2O4: Tb3+ nano-powders for forensic, anti-counterfeiting and optoelectronic devices. Inorganic Chemistry Communications 130, 108665.

Baatout, K., Saad, F., Baffoun, A., Mahltig, B., Kreher, D., Jaballah, N., Majdoub, M., 2019. Luminescent cotton fibers coated with fluorescein dye for anti-counterfeiting applications. Materials Chemistry and Physics 234, 304–310.

Hu, X., Yang, H.a., Guo, T., Shu, D., Shan, W., Li, G., Guo, D., 2018. Preparation and properties of Eu and Dy co-doped strontium aluminate long afterglow nanomaterials. Ceramics International 44 (7), 7535–7544.

Abdelhameed, M.M., Attia, Y.A., Abdelrahman, M.S., Khattab, T.A., 2021. Photochromic and fluorescent ink using photoluminescent strontium aluminate pigment and screen printing towards anti-counterfeiting documents. Luminescence 36 (4), 865–874.

Zhang, H., Chen, Z.-H., Liu, X., Zhang, F., 2020. A mini-review on recent progress of new sensitizers for luminescence of lanthanide doped nanomaterials. Nano Research, 1–15.

Ma, Q., Wang, J., Li, Z., Lv, X., Liang, L., Yuan, Q., 2019. Recent Progress in Time-Resolved Biosensing and Bioimaging Based on Lanthanide-Doped Nanoparticles. Small 15 (32), 1804969.

Calderón-Olvera, R.M., Albanés-Ojeda, E.A., García-Hipólito, M., Hernández-Alcántara, J.M., Álvarez-Perez, M.A., Falcony, C., Alvarez-Fregoso, O., 2018. Characterization of luminescent SrAl2O4 films doped with terbium and europium ions deposited by ultrasonic spray pyrolysis technique. Ceramics International 44 (7), 7917–7925.

Melo, B.C., Paulino, F.AA., Cardoso, V.A., Pereira, A.GB., Fajardo, A.R., Rodrigues, F.HA., 2018. Cellulose nanowhiskers improve the methylene blue adsorption capacity of chitosan-g-poly (acrylic acid) hydrogel. Carbohydrate polymers 181, 358–367.

Aminyan, R., Bazgir, S., 2019. Fabrication and characterization of nanofibrous polyacrylic acid superabsorbent using gas-assisted electrospinning technique. Reactive and Functional Polymers 141, 133–144.

Khattab, T.A., 2020. From chromic switchable hydrazones to smart materials. Materials Chemistry and Physics 123456.

Abumelha, H.M., 2021. Simple production of photoluminescent polyester coating using lanthanide-doped pigment. Luminescence 36 (4), 1024–1031.

Garrigue, Patrick, Marie-Hélène Delville, Christine Labrugère, Eric Cloutet, Pawel J. Kulesza, Jean Pierre Morand, and Alexander Kuhn. "Top− down approach for the preparation of colloidal carbon nanoparticles." *Chemistry of materials* 16, no. 16 (2004): 2984-2986.

Khattab, T.A., Tolba, E., Gaffer, H., Kamel, S., 2021. Development of electrospun nanofibrous-walled tubes for potential production of photoluminescent endoscopes. Industrial & Engineering Chemistry Research 60 (28), 10044–10055.

Devi, S., Avni Khatkar, V.B., Taxak, A.H., Sehrawat, P., Singh, S., Khatkar, S.P., 2020. Influence of Tb3+ doping on the structural and down-conversion luminescence behaviour of SrLaAlO4 nanophosphor. Journal of Luminescence 221, 117064.

Atta, A.M., 2021. Immobilization of silver and strontium oxide aluminate nanoparticles integrated into plasma-activated cotton fabric: luminescence, superhydrophobicity, and antimicrobial activity. Luminescence 36 (4), 1078–1088.

Carmona, N., Ortega-Feliu, I., Gomez-Tubio, B., Villegas, M.A., 2010. Advantages and disadvantages of PIXE/PIGE, XRF and EDX spectrometries applied to archaeometric characterisation of glasses. Materials Characterization 61 (2), 257–267.

Hill, G.T., Lee, D.T., Williams, P.S., Needham, C.D., Dandley, E.C., Oldham, C.J., Parsons, G.N., 2019. Insight on the Sequential Vapor Infiltration Mechanisms of Trimethylaluminum with Poly (methyl methacrylate), Poly (vinylpyrrolidone), and Poly (acrylic acid). The Journal of Physical Chemistry C 123 (26), 16146–16152.

Khattab, T.A., Fouda, M.MG., Abdelrahman, M.S., Othman, S.I., Bin-Jumah, M., Alqaraawi, M.A., Fassam, H.A., Allam, A.A., 2019. Development of illuminant glow-in-the-dark cotton fabric coated by luminescent composite with antimicrobial activity and ultraviolet protection. Journal of fluorescence 29 (3), 703–710.

Hameed, Ahmed, Enas Aljuhani, Tahani M. Bawazeer, Samar J. Almehmadi, Alia Abdulaziz Alfi, Hana M. Abumelha, Gaber AM Mersal, and Nashwa El-Metwaly. "Preparation of multifunctional long-persistent photoluminescence cellulose fibres." *Luminescence* 36, no. 7 (2021): 1781-1792.

Al-Qahtani, S., Aljuhani, E., Felaly, R., Alkhamis, K., Alkabli, J., Munshi, A., El-Metwaly, N., 2021. Development of Photoluminescent Translucent Wood toward Photochromic Smart Window Applications. Industrial & Engineering Chemistry Research.

Khattab, T.A., El-Aziz, M.A., Abdelrahman, M.S., El-Zawahry, M., Kamel, S., 2020. Development of long-persistent photoluminescent epoxy resin immobilized with europium (II)-doped strontium aluminate. Luminescence 35 (4), 478–485.